

IUHET-383
OHSTPY-HEP-E-98-003
February 1998

Top Quark Physics at Muon and other Future Colliders¹

M. S. Berger* and B. L. Winer†

**Department of Physics, Indiana University, Bloomington, Indiana 47405*

†*Department of Physics, Ohio State University, Columbus, Ohio 43210*

Abstract. The top quark will be extensively studied at future muon colliders. The threshold cross section can be measured precisely, and the small beam energy spread is especially effective at making the measurement useful. We report on all the activities of the top quark working group, including talks on top quark physics at other future colliders.

INTRODUCTION

The top quark is expected to be more sensitive than the lighter quarks to new physics effects. It is also the least accessible of the quarks due to its large mass. New colliders are under consideration that could considerably improve our understanding of the top quark.

The fact that the top quark is heavy and there are no heavier quarks (at least probably not) lends some credence to the idea that the top quark is special. Perhaps it is involved in the dynamics of electroweak symmetry breaking, or is subject to some new dynamics. Its Yukawa coupling is comparable in size to the gauge couplings and hence has a significant impact on the evolution of parameters with scale, and is a crucial ingredient in comparisons of weak-scale parameters with possible grand-unified theories. So it is important to measure the mass, couplings, and partial widths of the top quark as well as search for resonances in the $t\bar{t}$ spectrum. Any deviation from SM expectations would be of great interest.

Among the issues of paramount importance are (i) the nature of the absence of flavor changing neutral currents. This can be understood in the Standard Model (SM) with one Higgs boson as arising from the simplicity of the Model. Only one

¹) Summary report of the Top Quark Working Group at the Workshop on Physics at the First Muon Collider and at the Front End of a Muon Collider, November 6-9, 1997, Fermi National Accelerator Laboratory.

Higgs doublet does not allow tree-level effects (via the GIM mechanism) which are naturally there in almost any extension of the standard model. (ii) The test of QCD in a new regime, and the accurate measurement of its mass and couplings.

We summarize here the activities of the Top Quark Working Group [1]. Discussions highlighted the potential of muon colliders, while there were additional discussions on future electron-positron and hadron colliders. We refer the interested reader to the many recent reviews [2–6] of top quark physics for a more comprehensive treatment.

TOP-QUARK MASS MEASUREMENT AT THE $\mu^+\mu^- \rightarrow t\bar{t}$ THRESHOLD

One attractive feature of lepton colliders is the ability to do threshold cross section measurements. The W boson mass has been determined at LEP II by measuring the cross section $e^+e^- \rightarrow W^+W^-$ at the center-of-mass energy $\sqrt{s} = 161$ GeV. In general, accurate measurements of particles masses, couplings and widths are possible by measuring production cross sections near threshold. The possibility of measuring the top quark mass as well as other relevant parameters at a Next Linear Collider (NLC) has been under discussion for some years and was nicely reviewed for the group by Raja [7]. This technique has also been investigated more recently in the context of muon colliders. There is very rich physics associated with the $t\bar{t}$ threshold, including the determination of m_t , Γ_t ($|V_{tb}|$), α_s , and possibly m_h [8]. Ref. [7] contains a nice review of the most salient experimental measurements that can be done. This includes not only measurements of the mass and couplings of the top quark from the total cross section, but also extracting information from the various distributions of the detected particles. These issues carry over completely to the muon collider case, with some important differences in the characteristics of the collider beam having some impact on the sensitivities (see below).

Fadin and Khoze first demonstrated that the top-quark threshold cross section is calculable since the large top-quark mass puts one in the perturbative regime of QCD, and the large top-quark width effectively screens nonperturbative effects in the final state [9]. Such studies have since been performed by several groups [10–17]. The phenomenological potential is given at small distance r by two-loop perturbative QCD and for large r by a fit to quarkonia spectra.

The most important parameters affecting the shape of the threshold cross section are the top quark mass m_t and the strong coupling constant α_s . The mass determines at what energy the threshold turns on, while the strong coupling determines the binding between the $t\bar{t}$ pairs and hence causes in principle a resonance structure in the spectrum. However, since the top quark mass has turned out to be so large, only the $1S$ state appears as a structure on the threshold curve. The stronger the strong coupling, the tighter the binding and the lower the $1S$ peak occurs in energy. Weaker coupling also smooths out the threshold peak. These effects are

illustrated in Fig. 1. Clearly the effects of varying m_t and α_s are correlated; this fact necessitates that some kind of scan be performed of the threshold cross section.

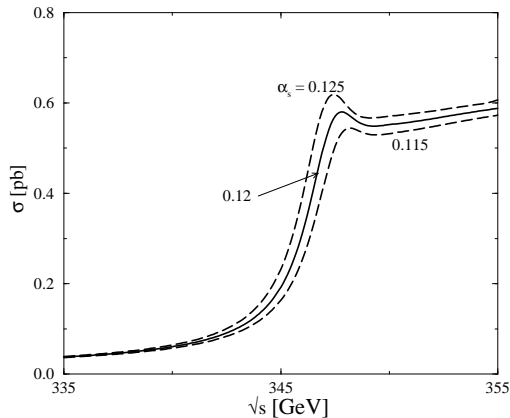


FIGURE 1. The cross section for $\mu^+\mu^- \rightarrow t\bar{t}$ production in the threshold region, for $m_t = 175$ GeV and $\alpha_s(M_Z) = 0.12$ (solid) and 0.115, 0.125 (dashes). Effects of ISR and beam smearing are included. This figure is from Ref. [18].

The scan can be optimized in various ways depending on the parameters one is most interested in measuring. In addition there is information contained in the various distributions of the final state particles. The momentum distribution of the top quark pairs as well as the forward-backward asymmetry are sensitive to the top quark width and α_s .

The presence of the Higgs boson affects the threshold curve. This contribution depends on the Higgs boson mass and the Yukawa coupling with which the Higgs boson couples to the top quark. The Yukawa coupling is fixed in the Standard Model for a given top quark mass, but could be different in extensions to the Standard Model. The Higgs boson contribution mainly affects the overall normalization of the threshold curve. Since the exchange of a light Higgs boson can affect the threshold shape, a scan of the threshold cross section can in principle yield some information about the Higgs mass and its Yukawa coupling to the top quark. Figure 2 shows the dependence of the threshold curve on the Higgs mass, m_h . However, it may be difficult to disentangle such a Higgs effect from two-loop QCD effects, which are not yet fully calculated [19]. Since one does not expect an accurate measurement of the Higgs mass from the $t\bar{t}$ threshold, one should properly think of the Higgs contribution as a systematic uncertainty that can be removed by measuring the Higgs mass and top quark Yukawa coupling elsewhere.

Beamstrahlung is the emission of radiation by one beam due to the action of the effective magnetic field of the other beam. This is expected to be an important issue at electron-positron colliders and clearly depends on the machine design. Muon colliders are expected to naturally have negligible beamstrahlung due to the large mass of the muon.

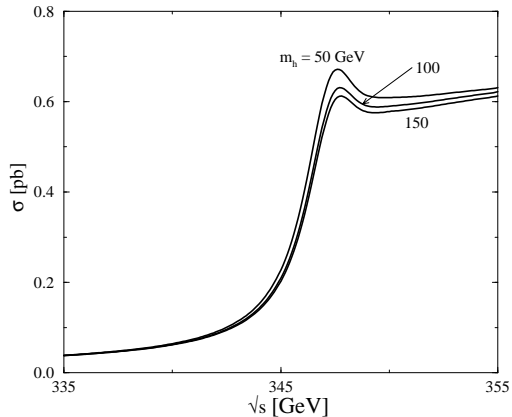


FIGURE 2. The dependence of the threshold region on the Higgs mass, for $m_h = 50, 100, 150$ GeV. Effects of ISR and beam smearing have been included, and we have assumed $m_t = 175$ GeV and $\alpha_s(M_Z) = 0.12$. This figure is from Ref. [18].

A more minor difference between the electron colliders and the muon colliders is the difference in the amount of initial state radiation (ISR). The expansion parameter is

$$\beta = \frac{2\alpha}{\pi} \left(\ln(s/m_\ell^2) - 1 \right), \quad (1)$$

where m_ℓ is the mass of the initial state particle (the electron or the muon). The radiator function that must be convoluted with the underlying cross section is

$$\mathcal{D}(x) = 1 + \frac{2\alpha}{\pi} (\pi^2/6 - 1/4) \left[\beta x^{\beta-1} \left(1 + \frac{3}{4}\beta \right) - \beta \left(1 - \frac{x}{2} \right) \right]$$

The ISR is reduced somewhat at a muon collider relative to an electron collider.

Two methods have been used to calculate the threshold cross section. The first (the coordinate-space approach) involves solving a nonrelativistic Schrödinger equation that splices together a QCD potential from perturbative QCD at small distance scales with one that is derived from fits to quarkonia spectra. The other method (the momentum space approach) involves solving a Bethe-Salpeter equation. The construction and the relationship between the QCD potentials used in each case is subject of recent study [20]. At a high luminosity muon collider it is evident that theoretical uncertainties in the threshold cross section might be the limiting factor in the ultimate obtainable precision.

The calculations used in simulations so far have been done mostly at the next-to-leading order (NLO) level. These next-to-next-to-leading order (NNLO) have not been taken into account even though their contributions can be important. For example, the $\mathcal{O}(\alpha_s^2)$ relativistic corrections can shift the location of the $1S$ peak by $m_t \alpha_s^4 \sim 150$ MeV and introduce a shift in the normalization of the total cross

section of order $\alpha_s^2 \sim 3\%$ [21]. Hoang described a procedure to calculate some of the NNLO corrections to the threshold cross section using NRQCD, an effective field theory of QCD for heavy quarks. NRQCD does away with the need for a phenomenological potential, and allows at least in principle the calculation of the cross section and all the distributions from the QCD Lagrangian.

The Abelian part (i.e. those contributions also present in QED) of the NNLO corrections calculated by Hoang are shown in Fig. 3. Notice that the corrections are a few percent and is fairly constant for the part of the cross section including and above the $1S$ peak, $E > -5$ GeV. (Compare the location of the peak in Fig. 1.)

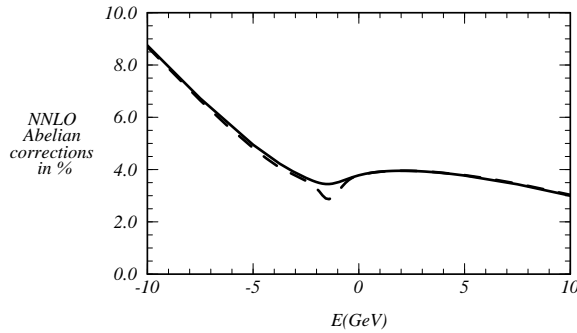


FIGURE 3. The NNLO Abelian corrections to the cross section for $\Gamma_t = 1.56$ GeV (solid line) and 0.80 GeV (dashed line), from Ref. [21].

Muon colliders are expected to naturally have a small spread in beam energy making them an ideal place to study the excitation curve. We present now the parameter determinations that are possible from measuring the total cross section near threshold at a $\mu^+\mu^-$ collider [18,22,23].

The beam energy spread at a $\mu^+\mu^-$ collider is expected to naturally be small. The rms deviation σ in \sqrt{s} is given by [24,25]

$$\sigma = (250 \text{ MeV}) \left(\frac{R}{0.1\%} \right) \left(\frac{\sqrt{s}}{350 \text{ GeV}} \right), \quad (2)$$

where R is the rms deviation of the Gaussian beam profile. With $R \lesssim 0.1\%$ the resolution σ is of the same order as the measurement one hopes to make in the top mass. For $t\bar{t}$ studies the exact shape of the beam is not important if $R \lesssim 0.1\%$. We take $R = 0.1\%$ here; the results are not improved significantly with better resolution².

Suppose one starts with the nominal values of $m_t = 175$ GeV and $\alpha_s(M_Z) = 0.12$. Assuming that 10 fb^{-1} integrated luminosity is used to measure the cross section at each energy in 1 GeV intervals, one can imagine obtaining the hypothetical sample

²⁾ The most recent TESLA design envisions a beam energy spread of $R = 0.2\%$ [26], and a high energy e^+e^- collider in the large VLHC tunnel would have a beam spread of $\sigma_E = 0.26$ GeV [27].

data, shown in Fig. 4. Cuts must be performed to eliminate the backgrounds; following Ref. [17] a 29% detection efficiency has been assumed for the signal where the W 's decay hadronically³ The data points can then be fit to theoretical predictions for different values of m_t and $\alpha_s(M_Z)$; the likelihood fit that is obtained is shown as the $\Delta\chi^2$ contour plot in Fig. 5. The inner and outer curves are the $\Delta\chi^2 = 1.0$ (68.3%) and 4.0 (95.4%) confidence levels respectively for the full 100 fb^{-1} integrated luminosity. Projecting the $\Delta\chi^2 = 1.0$ ellipse on the m_t axis, the top-quark mass can be determined to within $\Delta m_t \sim 70 \text{ MeV}$, provided systematics are under control. With an integrated luminosity of 10 fb^{-1} , the top-quark mass can be measured to 200 MeV.

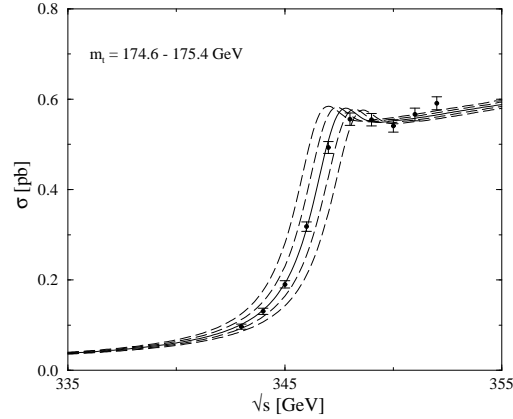


FIGURE 4. Sample data for $\mu^+\mu^- \rightarrow t\bar{t}$ obtained assuming a scan over the threshold region devoting 10 fb^{-1} luminosity to each data point. A detection efficiency of 29% has been assumed [17] in obtaining the error bars. The threshold curves correspond to shifts in m_t of 200 MeV increments. Effects of ISR and beam smearing have been included, and the strong coupling $\alpha_s(M_Z)$ is taken to be 0.12. This figure is from Ref. [18].

QCD measurements at future colliders and lattice calculations will presumably determine $\alpha_s(M_Z)$ to 1% accuracy (e.g. ± 0.001) [28] by the time muon colliders are constructed so the uncertainty in α_s will likely be similar to the precision obtainable at a $\mu^+\mu^-$ and/or e^+e^- collider with 100 fb^{-1} integrated luminosity. If the luminosity available for the threshold measurement is significantly less than 100 fb^{-1} , one can regard the value of $\alpha_s(M_Z)$ coming from other sources as an input, and thereby improve the top-quark mass determination.

There is some theoretical ambiguity in the mass definition of the top quark. The theoretical uncertainty on the quark pole mass due to QCD confinement effects is of order Λ_{QCD} , *i.e.*, a few hundred MeV [29,30]. For example, this theoretical ambiguity manifests itself in relating quark pole mass to other definitions of the top quark mass (such as the running top quark mass, $\overline{m}_t(\mu)$) that might be relevant as

³) This efficiency includes the decay branching fraction.

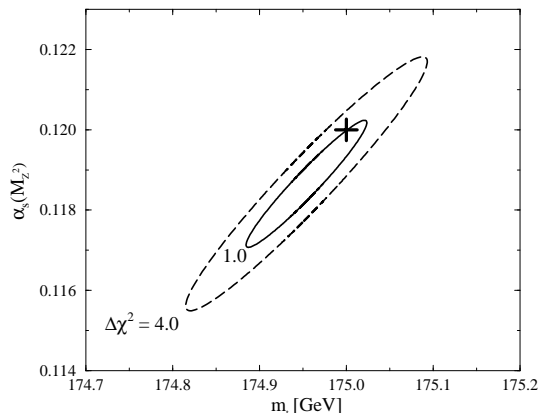


FIGURE 5. The $\Delta\chi^2 = 1.0$ and $\Delta\chi^2 = 4.0$ confidence limits for the sample data shown in Fig. 4. The “+” marks the input values ($m_t = 175$ GeV and $\alpha_s(M_Z) = 0.12$) from which the data were generated. This figure is from Ref. [18].

input to radiative correction calculations. So it is not clear that an extraction of the top-quark mass better than Λ_{QCD} is useful, at least at the present time.

Systematic errors in experimental efficiencies are not a significant problem for the $t\bar{t}$ threshold determination of m_t . This can be seen from Fig. 4, which shows that a 200 MeV shift in m_t corresponds to nearly a 10% shift in the cross section on the steeply rising part of the threshold scan, whereas it results in almost no change in σ once \sqrt{s} is above the peak by a few GeV. Not only will efficiencies be known to much better than 10%, but also systematic uncertainties will cancel to a high level of accuracy in the ratio of the cross section measured above the peak to measurements on the steeply-rising part of the threshold curve.

Differences of cross sections at energies below, at, and above the resonance peak, along with the location of the resonance peak, have different dependencies on the parameters m_t , α_s , m_h and $|V_{tb}|^2$ and should allow their determination. Consequently, the scan procedure described here can be further optimized for extraction of a particular parameter [18].

TOP QUARK PAIRS ABOVE THRESHOLD

The production of top quark pairs at energies above the threshold region at muon colliders will provide a great opportunity for searching for anomalous couplings and rare decays of the top quark. The production of top quarks can be used to test couplings to the neutral gauge bosons γ, Z in the production and to the W in the decays. An important new feature of top quark decays is the fact that the top quark decays before it has a chance to hadronize, so the spin information can be preserved from production to decay. This introduces the possibility that spin correlations between t and \bar{t} might even be measurable [31]. Finally a large sample

of top quark pairs allows us to search for possible rare decays, e.g. decays into a charged Higgs boson or flavor changing decays ($t \rightarrow c$) which are exceedingly small in the Standard Model.

The off-diagonal basis described by Parke [32] is superior to the standard helicity basis and allows one to describe the $t\bar{t}$ in their simplest possible terms. The basis is characterized by a spin angle ξ between the t spin and the \bar{t} momentum given by

$$\tan \xi = \frac{(f_{LL} + f_{LR})\sqrt{1 - \beta^2} \sin \theta^*}{f_{LL}(\cos \theta^* + \beta) + f_{LR}(\cos \theta^* - \beta)}, \quad (3)$$

where β is the top quark velocity, θ^* is the top quark scattering angle, and f_{IJ} is a combination of muon (or electron) and top quark couplings (see Ref. [31]). This spin basis interpolates between the beam direction at threshold and the top quark direction very far above threshold. Polarization of the incoming beams enhances the sensitivity to the basis choice. The dominant spin component's fraction of the total as function of the polarization of the beams is plotted in Fig. 6 Two different machines are included: the muon collider is assumed to have equal but opposite polarization for the μ^+ and μ^- beams; the NLC has only the electron beam polarized. A muon collider can do as well as an electron-positron machine with relatively less polarization.

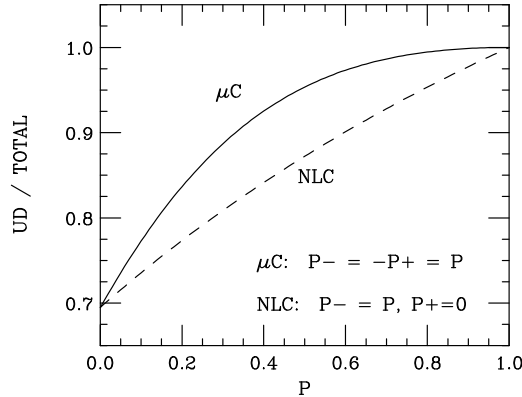


FIGURE 6. Fraction of the total cross section in the off-diagonal basis' Up-Down spin configuration as a function of the polarization. Both beams are assumed to be polarized for the Muon Collider (μC) but only one beam for the NLC. The plot is taken from Ref. [32].

In the future one hopes that detailed studies of the effects of anomalous coupling in the off-diagonal basis will become available. QCD corrections have been calculated and shown to be small [33]. If the muon or electron beams can be polarized, the sensitivity then to anomalous couplings can be enhanced [32].

Hoang described progress in two-loop calculations of the top production cross section in the kinematic region above the threshold [34]. His results for the part of the cross section do not yet include the axial pieces, but the one can see the

improvement in the stability under variations of the renormalization scale μ in Fig. 7.

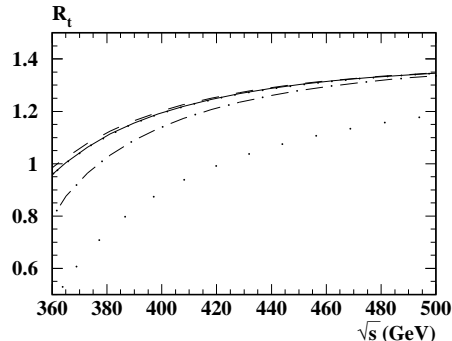


FIGURE 7. The total normalized photon-mediated cross section at the two-loop level versus \sqrt{s} for the renormalization scales $\mu = M_t$ (dashed), $\mu = 2M_t$ (solid) and $\mu = \sqrt{s}$ (dotted line), $M_t = 175$ GeV and $\alpha_s^{(5)}(M_z) = 0.118$. For comparison also the Born (wide dots) and the one-loop cross section for $\mu = 2M_t$ (dashed-dotted line) are displayed. To improve the stability under renormalization scale variations the known three-loop $\mathcal{O}(\alpha_s^3)$ in the large momentum expansion have been added to the two-loop cross section. The plot is taken from Ref. [34,35].

FLAVOR CHANGING NEUTRAL CURRENTS

There are strong phenomenological constraints on flavor changing neutral currents (FCNC) from K physics, for example. However, the possibility of FCNC in top couplings remains to be explored. Flavor changing decays of the top quark (e.g. $t \rightarrow c\gamma$) are extremely suppressed in the Standard Model, but new physics contributions could enhance the rate (see below and Ref. [36]). Another possible source of FCNC is to look for decays of Higgs bosons into single top quarks.

A unique feature of the muon collider is the ability to produce the Higgs boson in the s -channel [24,25]. This possibility arises because the Higgs boson coupling to leptons is proportional to their mass. Since the Higgs boson might be a very narrow object if one can center muon beams with very sharp beam profiles on the resonance energy one could produce a substantial sample of Higgs bosons and study their decays. An interesting set of decays are flavor changing ones, which for the Standard Model Higgs boson are completely absent. Many extensions to the Standard Model have flavor changing processes at the tree-level, and then the question becomes why they are so small in the physics that we see. If the Higgs boson is heavier than the top quark then one can consider the possibility that the Higgs boson decays via $H \rightarrow t\bar{c} + c\bar{t}$.

Reina and collaborators [37,38] chose a particular two-Higgs doublet model to provide examples of the kind of effects one might potentially see at a muon collider. The model is given by the Lagrangian

$$\mathcal{L}_Y^{(III)} = \eta_{ij}^U \bar{Q}_{i,L} \tilde{\phi}_1 U_{j,R} + \eta_{ij}^D \bar{Q}_{i,L} \phi_1 D_{j,R} + \xi_{ij}^U \bar{Q}_{i,L} \tilde{\phi}_2 U_{j,R} + \xi_{ij}^D \bar{Q}_{i,L} \phi_2 D_{j,R} + h.c. , \quad (4)$$

where η and ξ are non-diagonal Yukawa matrices. Usually at this point one imposes a discrete symmetry to eliminate tree-level FCNCs. Instead a reasonable choice is to assume that the flavor changing couplings adhere to the same hierarchy as the fermion masses [39]

$$\xi_{ij} = \lambda_{ij} \frac{\sqrt{m_i m_j}}{v} , \quad (5)$$

and tree-level FC couplings can be substantial for the top quark. This model (like all two Higgs doublet models) is parameterized by a mixing angle α between the two neutral scalars.

An important consideration for producing Higgs bosons in the s -channel, is the relative size of the beam width to the width of the Higgs boson [24,25]. A sufficiently sharp beam, if suitably tuned to the resonance energy, can take full advantage of the resonant cross section. One can define the effective cross section as the convolution of the Breit-Wigner σ_{tc}^{BW} cross section with a gaussian beam energy spread,

$$\sigma_{tc}^{eff} = \int d\sqrt{s'} \frac{\exp[-(\sqrt{s'} - \sqrt{s})^2/2\sigma^2]}{\sqrt{2\pi}\sigma} \sigma_{tc}^{BW}(s') , \quad (6)$$

where the rsm of the gaussian distribution is defined in terms of the parameter R .

In the analysis in Ref. [40] the effective cross section after convoluting with the beam width is expressed in units of $R_{\mu\mu}$ (not to be confused with the parameter R describing the beam width) as follows

$$R_{tc} = \frac{\sigma_{tc}^{eff}}{\sigma_0} = R(\mathcal{H}) (B(\mathcal{H} \rightarrow \bar{t}c) + B(\mathcal{H} \rightarrow \bar{c}t)) , \quad (7)$$

where $\sigma_0 = \sigma(\mu^+ \mu^- \rightarrow \gamma \rightarrow e^+ e^-)$ and $R(\mathcal{H}) = \sigma_{\mathcal{H}}/\sigma_0$ for $\sigma_{\mathcal{H}}$ the total cross section for producing \mathcal{H} .

As described above the results depend on how Γ_{h^0} compares to the resolution parameter R . This is shown in Fig. 8 which shows the results for the pure Breit-Wigner as well as different assumptions for R . Two choices for the mixing angle α shows the kind of variations one can get ($\alpha = 0$ means the s -channel Higgs h^0 does not couple to the gauge bosons which give competing decay channels $h^0 \rightarrow W^+ W^-, ZZ$).

With 1 fb^{-1} of integrated luminosity and gets around 100 $t\bar{c} + \bar{c}t$ events for $\alpha = 0$ and a few for $\alpha = \pi/4$ [40]. Clearly higher luminosity would be advantageous here.

Flavor changing rare decays of the top occur at an exceeding small rate in the Standard Model and the Minimal Supersymmetric Model (MSSM). However if R-parity violation occurs, then there is at least some hope that rare decays $t \rightarrow c$ could be detected at the upgraded Tevatron [41].

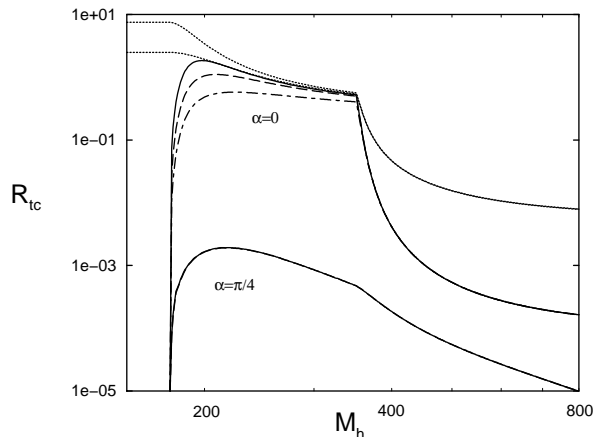


FIGURE 8. The value of $R(h^0)$ is shown as a function of M_{h^0} in a pure Breit-Wigner case (upper dotted line) and when the gaussian width distribution of the beam energy (for $R=0.01$) is taken into account (lower dotted line). The ratio R_{tc} is also shown for different values of the resolution parameter $R=0.001$ (solid), 0.01 (dashed) and 0.03 (dot-dashed), when $\alpha=0$ (upper group of curves) and when $\alpha=\pi/4$ (lower group of curves). This figure is from Ref. [40].

R-parity violation also could give an additional source of single top production. For example the lepton-number violating coupling⁴ λ' gives rise to the s -channel process

$$u\bar{d} \rightarrow \tilde{\ell} \rightarrow t\bar{b}. \quad (8)$$

The baryon-number violating coupling $\lambda'\prime$ gives rise to the s -channel processes

$$c\bar{d} \rightarrow \tilde{s} \rightarrow t\bar{b}, \quad (9)$$

$$c\bar{s} \rightarrow \tilde{d} \rightarrow t\bar{b}, \quad (10)$$

and the t -channel process

$$u\bar{d} \rightarrow t\bar{b}. \quad (11)$$

The prospects for setting bounds on R-parity violation from these processes is discussed in Refs. [41–43].

GLUON RADIATION

Top quark production involves gluon radiation because the top quark is a colored particle. In a hadron collider the gluon can arise in the initial and final states [44]. As far as gluon radiation at lepton colliders is concerned, there is no significant

⁴) For a definition and discussion of the R-parity violating couplings, see Refs. [42,43].

difference between $\mu^+\mu^-$ and e^+e^- colliders. There is no gluonic ISR, but the radiation must still be divided into production and decay stage radiation, i.e. the gluon can be thought of as originating off the produced t or \bar{t} , or it can be thought of as being among the decay products of the t or \bar{t} . Gluon radiation needs to be understood if we are able to do precise momentum reconstructions to obtain m_t , and also to identify top events by using mass cuts [45].

What one would really like to do is study the gluon radiation pattern. There are interference effects between the production and decay stage radiation that is potentially sensitive to the top quark width Γ_t . This occurs when the gluon energy is comparable to Γ_t . One such radiation pattern is shown in Fig. 9 for a particular kinematic configuration and a variety of values for Γ_t .

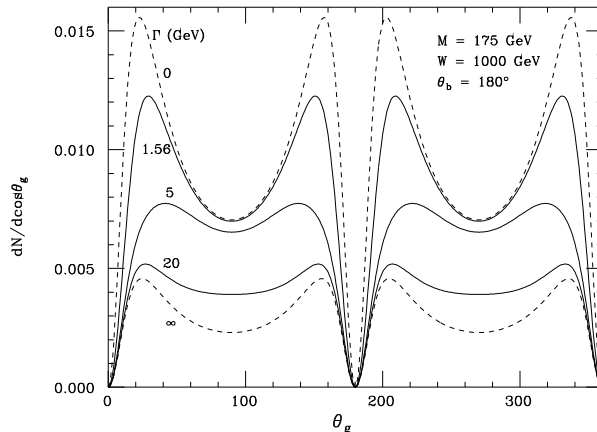


FIGURE 9. Soft gluon distribution in top production and decay at lepton colliders as described in the text, for t 's decaying to backward b 's and collision energy 1 TeV, from Ref. [45].

Whether one can really extract information about the top quark width by observing the interference patterns remains an open question [45]. The distributions that would be seen at a muon collider would involve all possible kinematic configurations. Moreover, the interference effects are much smaller for a 500 GeV collider which is more likely to be available first. Nevertheless, the interference is an interesting feature of QCD and one would like to see it even if it does not offer a new way to measure Γ_t .

TOP QUARK PHYSICS AT FUTURE HADRON COLLIDERS

Hughes [46] summarized top quark physics at future hadron colliders for the working group. He compared and contrasted the expected measurements at Run I of the Tevatron with what is expected at Run II, Tev33, and the LHC.

A possible manifestation of new physics is resonance structure in the $t\bar{t}$ mass distribution. The Tevatron is sensitive to both color singlet and color octet, while

at the LHC should be relatively insensitive to new color singlet gauge bosons (like Z') because gluon fusion is the dominant means of producing $t\bar{t}$ pairs.

Rare top decays ($t \rightarrow c$) are expected to be very small in the Standard Model due to the GIM mechanism and the competing (Cabibbo-allowed) decay $t \rightarrow b$. Branching fractions are typically of order 10^{-10} in the Standard Model, so the observation of rare decays of this sort indicates new physics. With 2 fb^{-1} , one should be able to get to the 10^{-3} level for $t \rightarrow c\gamma$ [46].

Observing single top production will become possible after the Tevatron upgrade. The single top production is proportional to the partial width $\Gamma(t \rightarrow Wb)$ and provides an expected precision of 16% for Run II and 9% for Tev33 [46]. Since the final state is a Wjj configuration rather than a $Wjjjj$ one, the background from QCD processes should be much higher than the usual $t\bar{t}$ case [36]. With 2 fb^{-1} , one should have roughly 100 events in the final sample.

DETECTOR AND BACKGROUND

Roser [47] described progress on a strawman detector for a muon collider and the interplay between the machine designers and detector designers. The detector backgrounds are actually more under control for the high energy (4 TeV) collider where most of the particles continue down the beam pipe without ever entering the detector.

While the total “background energy” does not depend on the energy of the beam, the “visible” background will depend on details of the lattice and the detector itself. There will be the usual collider backgrounds, such as beam halo, beam-beam, etc. Since backgrounds at a muon collider are expected to be large, one will want to use a large number of detector channels to achieve reasonable occupancies.

The following techniques are being used to study the detector: (1) lattice simulators COSY and MAD, (2) detector simulators MARS and GEANT, and (3) event generators LUND, PYTHIA, etc.

GEANT simulations yield radial particle fluxes per crossing for a layer of silicon at a radius of 10 cm:

$$\begin{aligned} 750 \text{ photons/cm}^2 &\rightarrow 2.3 \text{ Hits/cm}^2 \\ 110 \text{ neutrons/cm}^2 &\rightarrow 0.1 \text{ Hits/cm}^2 \\ 1.3 \text{ charged tracks/cm}^2 &\rightarrow 1.2 \text{ Hits/cm}^2 \\ \text{Total} &\rightarrow 3.7 \text{ Hits/cm}^2 \end{aligned}$$

This translates into a 0.4% occupancy in $300 \times 300 \mu\text{m}^2$ pixels. The corresponding numbers at a radius of 5 cm are 13.2 Hits/cm² for a 1.3% occupancy. The radiation dose in the silicon vertex detector at a 4 TeV muon collider at a radius of 10 cm is comparable to that of the LHC operating at $10^{34} \text{ cm}^{-2} \text{ s}^{-1}$ luminosity.

Backgrounds come from synchrotron radiation from electrons and from electromagnetic showering close to the detector. The lattice focuses the muons at the interaction point, so that the electrons cannot be kept in the beam pipe.

In summary, technology choices and detector optimization will require dedicated work. Because of the large backgrounds arising from the decaying muons, there will be pressure to compromise on 4π coverage.

CONCLUSION

An important issue regarding top physics at a muon collider is the amount of luminosity that would be available. Most of the signals presented here require significantly more than 1 fb^{-1} of integrated luminosity. The years ahead promise to be very exciting as we become able to study the top quark properties in more detail.

ACKNOWLEDGMENTS

We thank all the working group participants [1] for their contributions and discussion, and the conference organizers for an efficient and interesting workshop.

REFERENCES

1. Members of the working group: U. Baur, M. S. Berger, T. Bolton, E. Buckley-Geer, C. Campagnari, D. Chakraborty, D. Dominici, R. Drucker, A. Garren, E. Gottschalk, A. H. Hoang, R. Hughes, C. Kao, S. Keller, G. Landsberg, D. Miller, L. H. Orr, S. Parke, C. Quigg, R. Raja, L. Reina, R. Roser, Y. Shadmi, M. Smith, T. Stelzer, Z. Sullivan, G. Valencia, S. Vejcik, C. White, S. Willenbrock, B. L. Winer, G.-H. Wu, J. M. Yang.
2. *Future Electroweak Physics at the Fermilab Tevatron: Report of the TeV-2000 Study Group*, D. Amidei et al., Fermilab-Pub-96-082.
3. *Top Quark Physics: Future Measurements*, R. Frey et al., hep-ph/9704243.
4. S. Willenbrock, talk presented at 7th International Symposium on Heavy Flavor Physics, Santa Barbara, CA, 7-11 Jul 1997, hep-ph/9709355.
5. A. P. Heinson, talk presented at the 31st Rencontres de Moriond: QCD and High-energy Hadronic Interactions, Les Arcs, France, 23-30 Mar 1996, hep-ex/9605010.
6. T. Liss, talk presented at the International Europhysics Conference on High Energy Physics (HEP 95), Brussels, Belgium, 27 Jul - 2 Aug 1995, hep-ph/9510274.
7. R. Raja, these proceedings.
8. For a review on the top-quark physics near the threshold, see *e.g.*, J.H. Kuhn, TTP-96-18, lectures delivered at SLAC Summer Institute, Stanford, July, 1995.
9. V.S. Fadin and V.A. Khoze, JETP Lett. **46**, 525 (1987); Sov. J. Nucl. Phys. **48**, 309 (1988).
10. J. Feigenbaum, Phys. Rev. **D43**, 264 (1991).
11. W. Kwong, Phys. Rev. **D43**, 1488 (1991).
12. M. Strassler and M. Peskin, Phys. Rev. **D43**, 1500 (1991).

13. M. Jezabek, J.H. Kuhn and T. Teubner, *Z. Phys.* **C56**, 653 (1992); M. Jezabek and T. Teubner, *Z. Phys.* **C59**, 669 (1993); M. Jezabek, talk presented at *DESY-Zeuthen Workshop on Elementary Particle Theory: "Physics at LEP200 and Beyond"*, Teupitz, Germany, April 1994 (hep-ph/9406411); M. Jezabek, *Acta Phys. Pol.* **B26**, 789 (1995); J.H. Kuhn, *Acta Phys. Pol.* **B26**, 711 (1995).
14. G. Bagliesi, et al., *Workshops on Future e^+e^- Linear Colliders*, Hamburg, Germany and Saariselka, Finland, Sep 2–3 and Sep 9–11, 1991, CERN-PPE/92-05.
15. Y. Sumino, K. Fujii, K. Hagiwara, H. Murayama and C.-K. Ng, *Phys. Rev.* **D47**, 56 (1993); H. Murayama and Y. Sumino, *Phys. Rev.* **D47**, 82 (1993); Y. Sumino, *Acta Phys. Pol.* **B25**, 1837 (1994).
16. P. Igo-Kemenes, M. Martinez, R. Miquel and S. Orteu, CERN-PPE/93-200, Contribution to *the Workshop on Physics with Linear e^+e^- Colliders at 500 GeV*.
17. K. Fujii, T. Matsui and Y. Sumino, *Phys. Rev.* **D50**, 4341 (1994).
18. V. Barger, M.S. Berger, J.F. Gunion and T. Han, *Phys. Rev.* **D56**, 1714 (1997).
19. A. H. Hoang, *Phys. Rev.* **D56**, 5851 (1997); *Phys. Rev.* **D56**, 7276 (1997); and these proceedings.
20. M. Jezabek, et al., hep-ph/9801419.
21. A. H. Hoang, these proceedings, hep-ph/9712273.
22. M.S. Berger, talk presented at the *Workshop on Particle Theory and Phenomenology: Physics of the Top Quark*, Iowa State University, May 25–26, 1995, hep-ph/9508209.
23. M. S. Berger, these proceedings, hep-ph/9712486.
24. V. Barger, M.S. Berger, J.F. Gunion and T. Han, *Phys. Rev. Lett.* **75**, 1462 (1995).
25. V. Barger, M.S. Berger, J.F. Gunion and T. Han, *Phys. Reports* **286**, 1 (1997).
26. D. Miller, private communication.
27. J. Norem, private communication and <http://www-ap.fnal.gov/VLHC/electrons/index.html>.
28. P. N. Burrows *et al.*, SLAC-PUB-7371, to appear in *Proceedings of 1996 DPF/DPB Summer Study on New Directions for High-Energy Physics* (Snowmass 96), hep-ex/9612012.
29. M. C. Smith and S. Willenbrock, hep-ph/9612329.
30. M. Smith, these proceedings.
31. S. Parke and Y. Shadmi, *Phys. Lett.* **B387**, 199 (1996).
32. S. Parke, these proceedings, hep-ph/9802279.
33. J. Kodaira, T. Nasuno and S. Parke manuscript in preparation; M. Hori, Y. Kiyo, J. Kodaira, T. Nasuno and S. Parke, hep-ph/9801370.
34. A. H. Hoang, these proceedings, hep-ph/9712275.
35. K. G. Chetyrkin, A. H. Hoang, J. H. Kühn, M. Steinhauser and T. Teubner, hep-ph/9711327, to be published in *Z. Phys. C*.
36. T. Han, K. Whisnant, B. L. Young and X. Zhang, *Phys. Rev.* **D55**, 7241 (1997).
37. D. Atwood, L. Reina and A. Soni, *Phys. Rev.* **D53**, 1199 (1996); *Phys. Rev.* **D55**, 3156 (1997).
38. D. Atwood, L. Reina and A. Soni, *Phys. Rev. Lett.* **75**, 3800 (1995).
39. T.P. Cheng and M. Sher, *Phys. Rev.* **D35**, 3484 (1987); M. Sher and Y. Yuan, *Phys. Rev.* **D44**, 1461 (1991); A. Antaramian, L.J. Hall, and A. Rasin, *Phys. Lett.* **B69**, 1871 (1992); L.J. Hall and S. Weinberg, *Phys. Rev.* **D48**, R979 (1993).

40. L. Reina, these proceedings, hep-ph/9712426.
41. J. M. Yang, these proceedings.
42. A. Datta, J. M. Yang, B.-L. Young and X. Zhang, Phys. Rev. **D56**, 3107 (1997).
43. R. J. Oakes, et al., Phys. Rev. **D57**, 534 (1998).
44. V. A. Knoze, L. H. Orr, and W. J. Stirling, Nucl. Phys. **B378**, 413 (1992); L. H. Orr, T. Stelzer, and W. J. Stirling, Phys. Rev. **D52**, 124 (1995); Phys. Rev. **D56**, 446 (1997).
45. L. H. Orr, these proceedings, hep-ph/9802215.
46. R. Hughes, these proceedings.
47. R. Roser, these proceedings.